the sustained phase is believed to be mediated via store depletion-activated Ca^{2+} entry. Using patch-clamp recording and Ca^{2+} imaging, we show here that Ca_V channel currents, while found in spermatogenic cells, are not detectable in epididymal sperm and are not essential for the ZP-induced $[Ca^{2+}]_i$ changes. Instead, CATSPER channels localized in the distal portion of sperm (the principal piece) are required for the ZP-induced $[Ca^{2+}]_i$ changes. Furthermore, the ZP-induced $[Ca^{2+}]_i$ increase starts from the sperm tail and propagates toward the head.

Voltage-gated Ca Channels II

950-Pos Board B829

A Simple Link Between Gating And Pore Occupancy Can Describe Complex Ion-Dependent Kinetics Of Ca^{2+} Channels

Roman Shirokov, Anna Angelova, Alexandra Uliyanova.
New Jersey Medical School - UMDNJ, Newark, NJ, USA.

Several aspects of Ca^{2+} channel gating depend on permeant ions. These effects are difficult to describe in terms of regular ''states-and-rates'' models, which suggest that the channel does not change kinetic state(s) while it is open to pass current. We propose an approach to overcome this limitation. An open state is considered to have a minimum of two ''sub-states'': one is occupied by permeant ion and the other is not. The sub-states are allowed to have different kinetic paths of exit from the open state.

A minimalistic model of this sort explains the U-shaped voltage-dependence of inactivation by incorporating our previous finding that the apparent affinity of the channel pore for permeant ion increases during inactivation (Babich et al., JGP, 2007). The model implies that the tighter binding of permeant ions to the pore prevents current through inactivated channels, as if the pore is the ''inactivation gate''. This idea is in an apparent contradiction with the view that the mechanism of inactivation of Ca^{2+} currents, ''CDI'', is independent from that of Ba^{2+} currents, ''VDI'' (e.g., Barret and Tsien, PNAS, 2008). Here we show that our model describes well effects of molecular interventions that appear to differentially alter ''CDI'' and/or ''VDI''. Therefore, ion- and voltage-dependent components of inactivation may converge to act at the channel's pore.

951-Pos Board B830

Kinetic Modeling of CaV3.1

Katie C. Bittner[1], Lorin Milescu[2], Dorothy A. Hanck[1].
[1]University of Chicago, Chicago, IL, USA, [2]Harvard University, Boston, MA, USA.

T-type calcium channel kinetics have been well characterized at the macroscopic level, but less well so at the single channel level. The most thorough single channel kinetic analyses have been performed using recordings from native tissues where the specific isoform(s) present is unknown. As a result there is some discrepancy as to magnitude and voltage dependence of fundamental descriptors such as mean open time. It has been reported to be 0.5-2.5ms and either weakly voltage dependent or voltage independent (summarized in Perez-Reyes 2003). Macroscopic current measurements, on the other hand, are consistent with a voltage dependent O->C transition, suggesting that mean open time is voltage dependent. Bandwidth differences and other issues associated with signal to noise ratio for these conductance channels have no doubt contributed to measured durations. The development of gating models for these channels has been hampered by the paucity of high quality single channel data. Furthermore, previously published gating models of $Ca_V3.1$ correctly approximate the voltage dependence and time course of the macroscopic currents of $Ca_V3.1$ but fail to appropriately recapitulate the gating currents (Serrano et al 1999, Burgess et al 2002). We have utilized low noise recording methods to obtain higher bandwidth single channel data and paired it with maximum idealized point-likelihood analysis in QuB to estimate rate constants and their voltage dependence from single channel data for inclusion in developing models that correctly recapitulate macroscopic, single channel, and gating current data. Supported by F31-NS058334 (K.B.) and RO1-HL065680 (D.H.)

952-Pos Board B831

Voltage-sensor Pharmacology Of Voltage-activated Calcium Channels (cav)

Mirela Milescu, Kenton J. Swartz.
NIH/NINDS, Bethesda, MD, USA.

The four voltage sensors in Cav channels have distinct amino acid sequences, raising fundamental questions about their relative contributions to the function and regulation of the channel. Studies of Kv channels identified a S3b-S4 helix-turn-helix motif, termed paddle motif, which moves at the protein-lipid interface interface to drive activation of the voltage-sensors. This motif is an important pharmacological target for amphipathic neurotoxins and it has been suggested that is conserved in Cav and other voltage-gated ion channels. Here we show that the four S3b-S4 paddle motifs within the Cav channel could be transplanted into four-fold symmetric Kv channel to individually examine their contributions to the kinetics of voltage sensor activation and regulation by toxins.

953-Pos Board B832

Independent Contributions Of Segments IS6 And IIS6 To Activation Gating Of $Ca_V1.2$

Michaela Kudrnac[1], Stanislav Beyl[1], Annette Hohaus[1], Anna Stary[2], Thomas Peterbauer[1], Eugen Timin[1], **Steffen Hering**[1].
[1]Pharmacology and Toxicology, Vienna, Austria, [2]Institute for Theoretical Chemistry, Vienna, Austria.

Voltage dependence and kinetics of activation of $Ca_V1.2$ channels are affected by structural changes in pore lining S6 segments of the α_1-subunit. Significant effects on channel activation are induced by either proline or threonine substitutions in the lower third of segment IIS6 ('bundle crossing region'). Here we report that S435P in IS6 results in a large shift of the activation (−26mV) curve and slowed current kinetics. Threonine substitutions in positions Leu429 and Leu434 induced a similar kinetic phenotype with shifted activation curves.

Double mutations in segments IS6 and IIS6 induced additive shifts of the activation curves, e.g.: L429T/I781T (-44.0 ± 1.0), L434T/I781T (-50.3 ± 0.8), L429T/L779T (-22.5 ± 0.8) and L434T/L779T (-32.3 ± 0.8). If the gating sensitive residues in the two neighboring segments IS6 and IIS6 do not interact then the change in free energy (ΔG_{double}) of the double mutant is equal to the sum of the changes in free energy of the two single mutations ($\Delta G_{mut\ IS6}$ and $\Delta G_{mut\ IIS6}$ see scheme, see also Horovitz 1996). Double mutant cycle analysis revealed that the studied IS6 and IIS6 mutations are energetically independent and thus have independent impacts on activation gating.

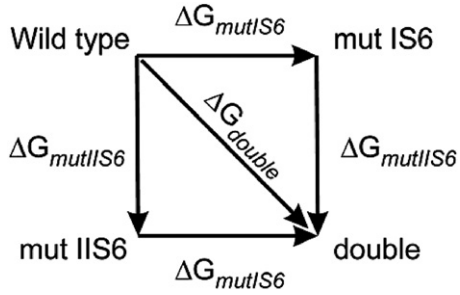

Supported by FWF-Project P19614-B11.

954-Pos Board B833

Role of S4 segments in Ca_v1 and Ca_v3 channels: gating and current density

Juan F. Higueldo-Garcia, Jonatan Barrera-Chimal, Juan C. Gomora.
Institute of Cell Physiology, UNAM, Mexico City, Mexico.

Gating of voltage-dependent calcium channels (Ca_v) is determined by S4 segments in each of the four α1-subunit domain's. In the S4 segments, also known as voltage sensors, every third position there is a positive charged residue (lysine or arginine). However, both high-voltage (HVA) and low-voltage (LVA or T-type) activated Ca_v channels, show S4 segments with very similar sequences. This issue had already been investigated in some members of T-type Ca_v3 family, mainly in $Ca_v3.1$ (α1G), and one report on $Ca_v3.2$ (α1H), but there is no data on the $Ca_v3.3$ (α1I). To investigate the role of S4 segments in the differences in gating between $Ca_v3.3$ and $Ca_v1.2$ we made a chimerical approach swapping the S4 segment of domain II of $Ca_v3.3$ with the corresponding S4 segment of $Ca_v1.2$. We have used HEK-293 cells and the whole-cell patch clamp technique to characterize the functional expression of the constructs. Our preliminary results indicate that the substitution of the IIS4 segment of $Ca_v3.3$ for that of $Ca_v1.2$ induce a 25 mV positive shift in the *I-V* peak with respect to the $Ca_v3.3$ wild type (WT). Also, the Boltzmann parameters were significantly different between the WT and the chimeric channel *I-V* curves. There was no appreciable change in the kinetics of the currents. An unexpected result was a drastic decrease (< 95%) in the current density of the chimeric channel. A possible explanation is that the IIS4 (the whole or some residues of it) of $Ca_v1.2$ is interacting with the rest of the channel protein in such way that makes more stable the closed state of the channel. Additional experiments are under way to further study this observation.

This work was supported by CONACYT México J50250Q.

955-Pos Board B834

Depolarization-induced Potentiation Of Cav1.1 Does Not Require The Distal C-terminus

Joshua D. Ohrtman, Kurt G. Beam.
University of Colorado Health Sciences Center, Denver, CO, USA.

In adult skeletal muscle, the majority of the L-type Ca^{2+} channel CaV1.1 subunit is truncated post-translationally at residue 1664 (PNAS, 102:5274-79), raising the question of the functional role of the distal residues (1665-1873). It has been suggested (J Neurosci.17:1243-55; J Biol Chem. 277:4079-87) that (i) the distal C-terminus is non-covalently associated with the remainder of the channel, (ii) reduces channel open probability, and (iii) loses this inhibitory effect as a result of phosphorylation during strong depolarization. In regard to point (ii), previous analysis of L-type ionic conductance (G) and

membrane gating charge movements (Q) demonstrated that channel open probability (i.e., G/Q ratio) was indistinguishable for full-length or truncated (at 1662) CaV1.1 expressed in *dysgenic* myotubes (Nature 360:169-171). Here we have investigated the effects of removing the distal C-terminus on depolarization-induced potentiation of CaV1.1. Specifically, tail currents were measured for repolarization to -30 mV following a 200 ms depolarization to either +40 or +90 mV. For both full-length and truncated CaV1.1, tail currents were both larger (~2.5-fold) and more slowly decaying (~2-fold) following the +90 mV depolarization. Thus, we find no evidence for a role of the CaV1.1 distal C-terminus in depolarization-induced potentiation.

We are currently examining the role of the CaV1.2 distal C-terminus by co-expression of full-length or truncated (1669) CaV1.2 in tsA-201 cells together with β_{2a} and $\alpha_2\delta 1$. In agreement with previous work (J Physiol. 576:87-102, and in contrast to CaV1.1, truncation of CaV1.2 resulted in ~4-fold increase in the G/Q ratio. We are currently investigating the ability of the truncated CaV1.2 to undergo depolarization-induced potentiation. Supported by NIH (NS24444) and MDA grants to KGB.

956-Pos Board B835

Chimera of CaV1.2 and CaV3.1 alpha1 Subunits Suggests Role of the C-terminal Tail in Cytosolic Mg2+ Actions on CaV1.2 Gating

Min Wang[1], Yoganand Yadari[2], **Joshua R. Berlin[2]**.
[1]Emisphere Technologies, Tarrytown, NY, USA, [2]UMDNJ-New Jersey Medical School, Newark, NJ, USA.

Previous studies (Wang and Berlin, *Am. J. Physiol*. **291**:C83, 2006) have shown that gating properties of $Ca_V1.2$ channels (subunits α_1, β_{2A} and $\alpha_2\delta$) expressed in tsA201 cells are significantly altered by varying cytosolic Mg^{2+} across a range of physiologic concentrations. Alterations in gating include changes in peak current amplitude as well as kinetics of current inactivation. In contrast, when $Ca_V3.1$ (α_1 subunit only) is expressed, varying cytosolic Mg^{2+} across a similar concentration range has little or no effect on channel gating. To understand the molecular basis for the effects of cytosolic Mg^{2+} on these related Ca^{2+} channels, a chimera channel consisting of $Ca_V3.1$ (α_1 residues 1-1826) with the C-terminal region of $Ca_V1.2$ (α_1 residues 1515-2171) was constructed and expressed in tsA201 cells. Ca^{2+} currents were measured in cells whole-cell patch-clamped with electrodes containing salt solutions in which Mg^{2+} and Ca^{2+} concentrations were strongly buffered. The chimera Ca^{2+} channel had a similar membrane potential dependence for activation and steady-state inactivation as $Ca_V3.1$; however, the rate of current inactivation was slowed at least two-fold. Varying patch electrode Mg^{2+} concentration had little effect on the rate of current inactivation, similar to $Ca_V3.1$, but unlike $Ca_V1.2$. On the other hand, current amplitude was depressed in the chimera channel with increasing Mg^{2+}. These results show that the C-terminal tail of $Ca_V1.2$ affects kinetics of channel gating. At least in part, changes in channel availability with cytosolic Mg^{2+} can be attributed to the C-terminal tail of $Ca_V1.2$; however, this domain alone cannot be responsible for Mg^{2+}-dependent regulation of channel gating kinetics.

957-Pos Board B836

$Ca_V1.4$ C-tail Segment (ICDI) Inhibits Ca_V Channel Inactivation by Competing with Calmodulin–Resolution by Holochannels and Calmodulin FRET Sensors

Xiaodong Liu, Philemon S. Yang, Vincent Wu, Wanjun Yang, David T. Yue.
Johns Hopkins University, Baltimore, MD, USA.

An intriguing variation on calmodulin/Ca_V channel inactivation (CDI) is the action of a C-tail segment from $Ca_V1.4$ channels (ICDI) to eliminate CDI. Introducing ICDI into $Ca_V1.2$ or $Ca_V1.3$ channels nearly abolishes strong baseline CDI, and a like effect is observed when ICDI is present within $Ca_V1.4$ itself. In retina, the effect in $Ca_V1.4$ helps sustain Ca^{2+} influx despite maintained depolarization. Contrasting with clear-cut function, the underlying ICDI mechanism remains controversial. One group proposes that ICDI allosterically inhibits CDI (Wahl-Schott *et al* PNAS 2006), while another suggests direct competition between calmodulin and ICDI for the channel (Singh *et al* Nature Neurosci 2006). The discussion hinges on differing calmodulin versus channel peptide assays. Here, we perform functional interaction assays using holochannels within live cells. As baseline, we electrophysiologically characterized $Ca_V1.3$ channels fused to an ICDI-containing segment ($\alpha_{1D\text{-}ABI\text{-}F}$). These $\alpha_{1D\text{-}ABI\text{-}F}$ channels exhibited little CDI compared to wild-type $Ca_V1.3$. Critically, variations in the ambient calmodulin concentration would only affect competitive versus allosteric mechanisms. Indeed, when calmodulin was depleted by a 'calmodulin sponge,' residual CDI in $\alpha_{1D\text{-}ABI\text{-}F}$, was totally eliminated. More telling, when calmodulin was over-expressed with $\alpha_{1D\text{-}ABI\text{-}F}$, we observed a resurgence of CDI to wild-type $Ca_V1.3$ levels. To test for precise agreement with a competitive mechanism, we co-expressed $\alpha_{1D\text{-}ABI\text{-}F}$ channels with BSCaMIQ, a FRET biosensor of calmodulin (Black *et al* Biochemistry 2006). Accordingly, both CDI and calmodulin concentrations could be measured within single cells; and pooling data from cells exhibiting variable calmodulin levels permitted explicit resolution of an *in situ* calmodulin binding curve, in strict agreement with a competitive mechanism. In all, ICDI suppresses CDI by competing with calmodulin for the channel, raising the possibility that natural variations in calmodulin might customize CDI through this mechanism.

958-Pos Board B837

Structure-function Relationship of N-terminal Deletion Mutants of Cardiac L-type Calcium Channel ß1-subunits

Wanchana Jangsangthong[1], Elza Kuzmenkina[1], Ismail F.Y. Khan[1], Roger Hullin[2], Stefan Herzig[1].
[1]University of Cologne, Cologne, Germany, [2]University Hospital Bern, Bern, Switzerland.

Auxiliary ß-subunits of L-type Ca2+ channel (L-VDCC) profoundly modulate properties of L-VDCC. Previously, we demonstrated that the N-terminus of ß2-subunit serves as a length-dependent structural determinant of channel inactivation (Herzig et al., FASEB J. 2007). Here, we tested the role of the N-terminus of ß1a-subunit. Three artificial ß1a-subunit mutants with different N-terminus lengths, ß1aN18, ß1aN27 and ß1aN51, were created. Their modulatory functions were investigated in recombinant L-VDCC and compared with the natural full-length isoform, termed ß1aN60.

In whole-cell patch-clamp measurements, we confirmed functional expression of all ß1a-subunit isoforms by a marked increase of current density and a leftward shift of activation, as compared to control transfections without any ß-subunit. No obvious differences were found among ß1a-subunit isoforms. In contrast, shortenening of the N-terminus progressively decreased the rate and extent of time-dependent inactivation at all test voltages.

Descriptive analysis of the single-channel data (e.g., peak ensemble average current, open probability, availablility) revealed similar parameters among ß1a-subunit isoforms, except for small deviations with ß1aN51. Strikingly, the extent of the inactivation of ensemble average currents followed the length of the N-terminus (ß1aN60>ß1aN51>ß1aN27>ß1aN18). For more detailed kinetic analysis, we performed Markov modeling using the scheme:

C-C-C-C-C-O

Ic-Ic-Ic-Ic-Ic-Io

with the rate constants for C-C and Ic-Ic: alpha, beta; C-O and Ic-Io: alphá, betá; C-I and O-I: gamma, delta. Channel open probability, availability, and first-latency, open-time and closed-time histograms were well fitted simultaneously. We found significant linear correlation between the inactivation rates gamma and delta and the N-terminus length. The other parameters alpha, alphá, beta, betá) did not vary with the N-terminal length of the ß1a-subunit.

Our results demonstrate that inactivation is under length-dependent control of the N-terminus of L-VDCC ß1-subunit. This could represent a general mechanism of ß-subunit modulation.

959-Pos Board B838

Modulation Of Calcium Currents By Acidic Domains Of Calcium Channel Subunits: A Novel Feedback Mechanism?

Vicenta Salvador-Recatala, Robert M. Greenberg.
University of Pennsylvania, Philadelphia, PA, USA.

Voltage-gated calcium (Cav) channels are essential to the function of excitable cells. Cav channels are multimeric proteins that consist of a pore forming subunit (alpha1) and several accessory subunits. We are characterizing an accessory beta subunit from the human pathogen Schistosoma mansoni (SmCavbeta), using a human alpha1E channel (Cav2.3) as the modulatory substrate and the whole-cell patch-clamp technique. SmCavbeta modulates Cav2.3 currents in a conventional manner, but it induces them to run-down to ~75% of their initial amplitudes within two minutes of establishing the whole-cell configuration. SmCavbeta has a unique poly-acidic motif of 15 aspartate and glutamate residues in its N-terminus. A mutant version of SmCavbeta lacking the first forty-six amino acids, which comprise the entire poly-acidic motif, did not induce run-down of the calcium current. Smaller deletions of this region provide a higher-resolution profile of the structures required for run-down. A deletion of the N-terminus that eliminates the amino acids preceding the acidic motif reduces the Ca2+ current to the same extent as the wild type subunit, by ~29% within 4 minutes of patch disruption. A deletion that eliminates the first six residues of the poly-acidic motif also reduces the calcium current significantly, but to a lesser extent than the wild-type subunit (by ~17% within the same time-frame). A deletion mutant subunit without the first nine acidic residues of the poly-acidic motif did not induce run-down. Based on the structural homology between the poly-acidic motif of SmCavbeta and that of calcium binding phosphoproteins, we speculate that SmCavbeta binds Ca2+. Since similar N-terminal poly-acidic motifs are found in all platyhelminths examined, it is tempting to hypothesize that these structures represent a feedback mechanism that modulates influx of extracellular Ca2+ into the excitable cells of platyhelminths.